ORIGINAL PAPER

Enhanced cycling performance of spinel LiMn$_2$O$_4$ coated with ZnMn$_2$O$_4$ shell

Xifei Li · Youlong Xu

Abstract ZnMn$_2$O$_4$ shell-coated LiMn$_2$O$_4$ was prepared by a simple routine that the mixture of LiMn$_2$O$_4$ and ZnO were heated at 750 °C. The structure and electrochemical performance of as-prepared powder compared with the pure LiMn$_2$O$_4$ were characterized by X-ray diffraction (XRD), scanning electron microscopy (SEM), energy dispersive spectrometry (EDAX), and galvanostatic charge–discharge testing, respectively. The results of XRD, SEM, and EDAX show that ZnMn$_2$O$_4$ is formed on the surface of LiMn$_2$O$_4$ particles. Charge–discharge testing reveals that ZnMn$_2$O$_4$ shell-coated LiMn$_2$O$_4$ greatly enhances the capacity retention of the spinel LiMn$_2$O$_4$. Furthermore, the modified LiMn$_2$O$_4$ shows significant enhancement in cycling stability at rates from 0.5 C to 12 C. It is found that the improved cycling performance and rate capability of the modified LiMn$_2$O$_4$ are attributed to the effective decrease of manganese dissolution from spinel structure because of ZnMn$_2$O$_4$ shell coated on the surface of LiMn$_2$O$_4$ particle.

Keywords ZnMn$_2$O$_4$ shell · Capacity retention · Rates capability · Manganese dissolution

Introduction

Due to its low cost and low toxicity, the spinel LiMn$_2$O$_4$, the cathode for Li-ion batteries, has been extensively investigat-ed. The spinel LiMn$_2$O$_4$ has a cubic structure with the space group of Fd3m symmetry in which lithium and manganese ions occupy tetrahedral (8a) sites and octahedral (16d) sites, respectively, within a cubic close-packed oxygen array with oxygen ions in 32e sites. Many reports revealed that the spinel LiMn$_2$O$_4$ offers a potentially attractive alternative to the presently commercialized LiCoO$_2$. However, a key problem prohibiting LiMn$_2$O$_4$ from commercialization is its severe capacity fading during cycling [1].

There are several factors that cause capacity fade of spinel LiMn$_2$O$_4$, as it had been reported by many investigators [2–5]. During cycling, Mn can dissolve into the electrolyte according to the disproportionation equation ($2Mn_{solid}^{3+} \rightarrow Mn_{solid}^{4+} + Mn_{solution}^{2+}$) [4]. To minimize Mn dissolution into electrolyte solution, an effective strategy, coating the spinel LiMn$_2$O$_4$ particles with organic and inorganic compounds, has been investigated [6–8]. Ha et al. [7] coated LiMn$_2$O$_4$ spinel with CeO$_2$ and improved the cyclability of the spinel LiMn$_2$O$_4$ cathode materials. Chan et al. [8] reported that Li$_2$O–2B$_2$O$_3$ glass was coated on the surface of spinel LiMn$_2$O$_4$, which showed better cyclability than the pure one.

In this study, for the fist time, we coated the spinel LiMn$_2$O$_4$ with ZnMn$_2$O$_4$ shell. The modified LiMn$_2$O$_4$ can be protected from Mn dissolution, as the shell of ZnMn$_2$O$_4$ is formed on the surface of the spinel LiMn$_2$O$_4$ particles. Therefore, it is expected that the modified LiMn$_2$O$_4$ shows the excellent cycle performance.

X. Li · Y. Xu (✉)
School of Electronic and Information Engineering,
Xi'an Jiaotong University,
Xi'an 710049, China
e-mail: ylxu@mail.xjtu.edu.cn

Experimental

Spinel LiMn$_2$O$_4$ powder was prepared by a solid-state reaction. A mixed fine powder of Li$_2$CO$_3$ and MnCO$_3$ in 1:4 mole ratio was heated at 600 °C for 6 h, then calcined at

750 °C in air for 72 h with intermittent grinding. As-prepared $LiMn_2O_4$ and ZnO (2 wt%) were mixed in the ball mill for 12 h. Then, the well-mixed powders were calcined at 750 °C for 2 h in air, followed by slow cooling to room temperature.

The spinel electrode was fabricated from a slurring mixture containing 70 wt% active material, 20 wt% acetylene black, and 10 wt% polyvinylidene fluoride binder in *N*-methylpyrrolidinone solvent. The slurry was coated on an aluminum foil, followed by drying in a vacuum oven at 120 °C for 48 h, and an electrode was formed.

The CR-2016-type coin cells were assembled in Mikrouna Super (1225/750) glove box under a dry argon atmosphere. $LiMn_2O_4$ electrode is used as positive electrode and Li sheet as negative electrode. Electrolyte was 1 M $LiPF_6$ dissolved in ethylene carbonate (EC)/diethyl carbonate (DEC)/ethyl methyl carbonate (EMC) in a 1:1:1 volume ratio (Dongguan Shanshan Battery Materials).

X-ray diffraction (XRD) analysis was performed with a Rigaku D/MAX-2400 diffractometer (Rigaku), using Cu-Kα radiation (λ =0.154056 nm). Scanning electron microscope (SEM) and energy dispersive spectrometry (EDAX) were taken with a JSM-6700F (JEOL). Charge–discharge characteristics were tested galvanostatically between 3.5 and 4.3 V (vs Li/Li$^+$) at room temperature by LAND Battery Test System.

Results and discussion

The XRD patterns of pure $LiMn_2O_4$ and modified $LiMn_2O_4$ are showed in Fig. 1. In case of the pure $LiMn_2O_4$, only a single phase of spinel structure is observed. Some additional peaks for $ZnMn_2O_4$ can be observed for the modified $LiMn_2O_4$, but no peaks corresponding to the phase of ZnO. For the modified $LiMn_2O_4$ resulting from the calcinations of $LiMn_2O_4$ particle with ZnO at 750 °C for 2 h, we suppose that the zinc oxide reacts with $LiMn_2O_4$ to form $ZnMn_2O_4$ shell on the surface of $LiMn_2O_4$ particles. The lattice parameters of pure $LiMn_2O_4$ and modified $LiMn_2O_4$ were calculated from the XRD spectrum. They are 0.824577 and 0.824521 nm, respectively. No change in lattice parameter indicates that Zn^{2+} does not dope the spinel structure; that is, no phase of $Li_{1-x}Zn_xMn_2O_4$ or $LiZn_xMn_{2-x}O_4$ is formed.

A series of SEM micrographs, in Fig. 2, reveals the morphological changes that occurred during the process of modifying spinel $LiMn_2O_4$. As it is shown in Fig. 2a, the pure $LiMn_2O_4$ had obvious visible fringes, indicating that the crystals of spinel $LiMn_2O_4$ grow very well and have good crystallinity. After mixing $LiMn_2O_4$ and ZnO in the ball mill, in Fig. 2b, it clearly exhibits that the fine powders of ZnO distributed uniformly on the surfaces of $LiMn_2O_4$ particles. After heat treatment, however, no individual zinc

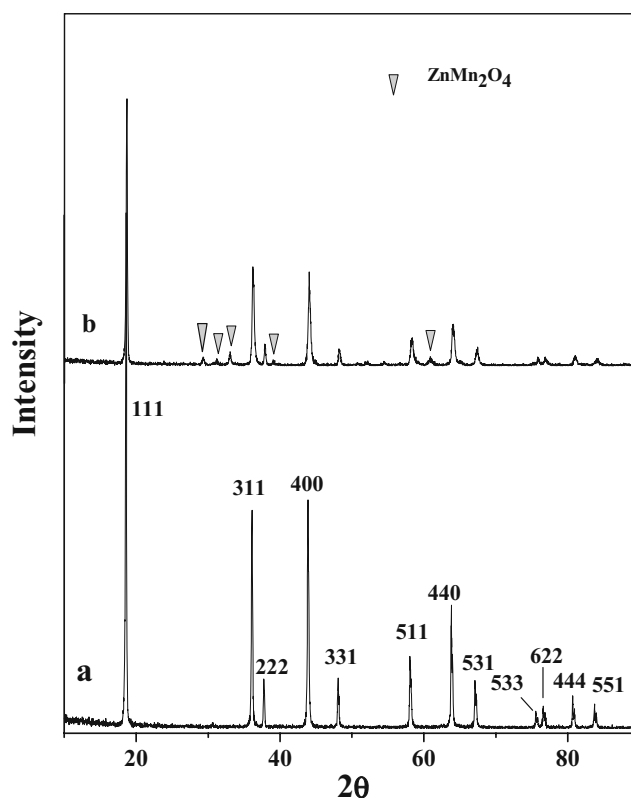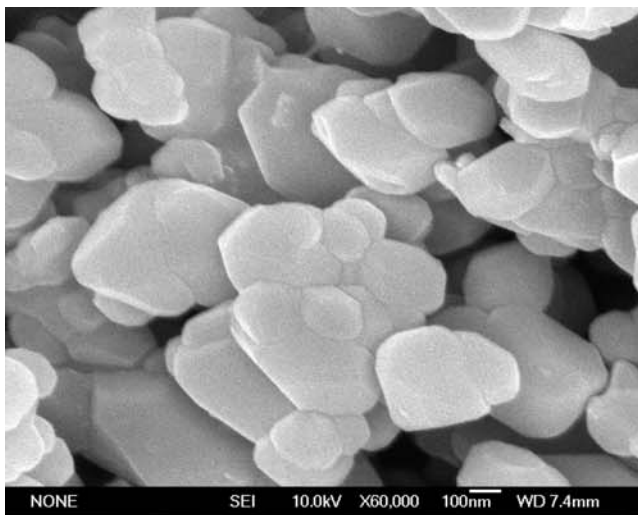**Fig. 1** XRD patterns of **a** pure $LiMn_2O_4$ and **b** modified $LiMn_2O_4$

oxide particles are visible, which is in good agreement with the result of XRD. The surfaces of modified $LiMn_2O_4$ particles are smooth with a similar morphology of the pure $LiMn_2O_4$ particles. It is indicated that ZnO particles reacted with spinel $LiMn_2O_4$ particles and formed a shell of $ZnMn_2O_4$ on the surface of $LiMn_2O_4$ particles.
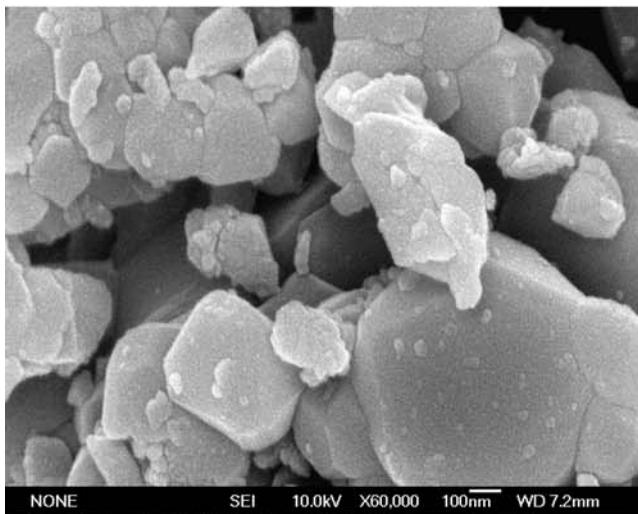
To confirm the composition of modified $LiMn_2O_4$ powder, EDAX analysis was performed and shown in Fig. 3. Zinc can be clearly observed on the surface of modified $LiMn_2O_4$. EDAX analysis thus reveals the evidence for the formation of $ZnMn_2O_4$ on the surface of modified $LiMn_2O_4$.

Figure 4 shows the TEM image of the cross-sections of the spinel $LiMn_2O_4$ without (a) and with (b) modification, respectively. Obviously, in the case of modified $LiMn_2O_4$, a shell of $ZnMn_2O_4$ is coated on the surface of $LiMn_2O_4$ particles, while no shell for pure one. The zinc oxides disappear due to reactions with spinel $LiMn_2O_4$, forming $ZnMn_2O_4$ shell on the surface of $LiMn_2O_4$ particles. This observation reveals that the shell/core particles were formed after the modification.
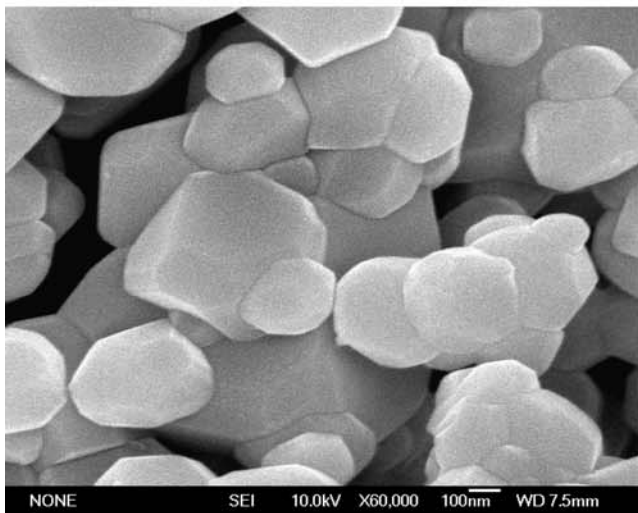
After charged and discharged galvanostatically for ten cycles, the assembled cells were stored at 60 °C for a week. Figure 5 shows the discharge curves of pure $LiMn_2O_4$ and modified $LiMn_2O_4$ before and after storage. The pure $LiMn_2O_4$ showed 18.2% capacity loss after storage at 60 °C for a week, while the modified $LiMn_2O_4$ showed 2.7% capacity loss. It is clear that the decrease of discharge
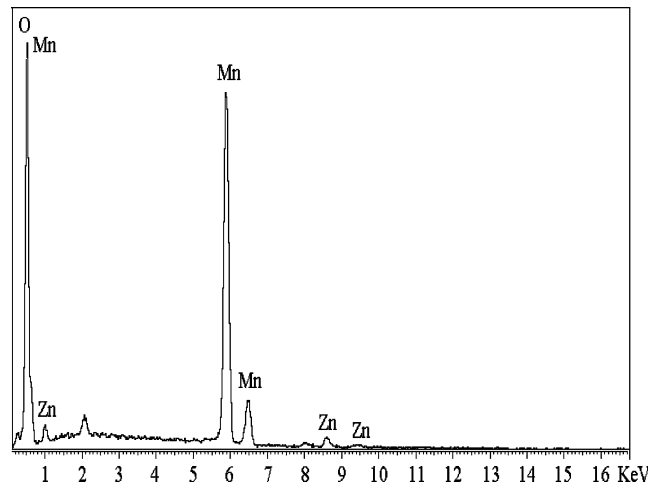
a

Fig. 3 EDAX analysis of modified $LiMn_2O_4$
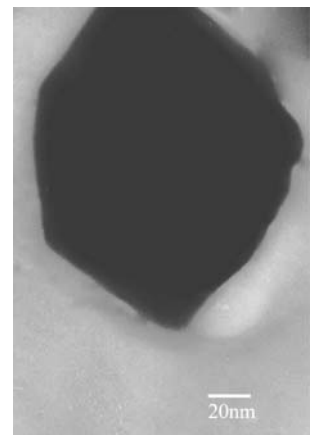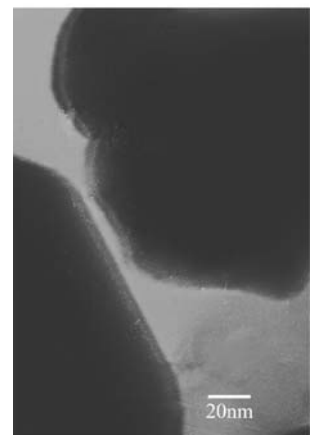
capacity of pure $LiMn_2O_4$ before and after storage is severer than that of modified $LiMn_2O_4$. This obvious decrease of discharge capacity is due to Mn dissolution into the electrolyte solution [9]. Therefore, the modified $LiMn_2O_4$ effectively diminished the Mn dissolution into the
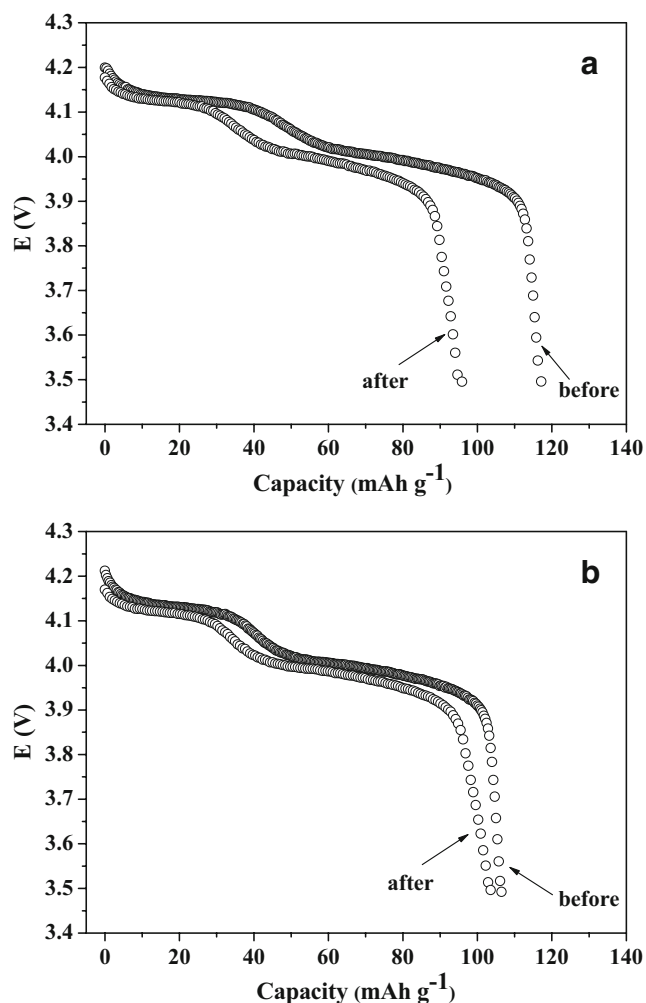
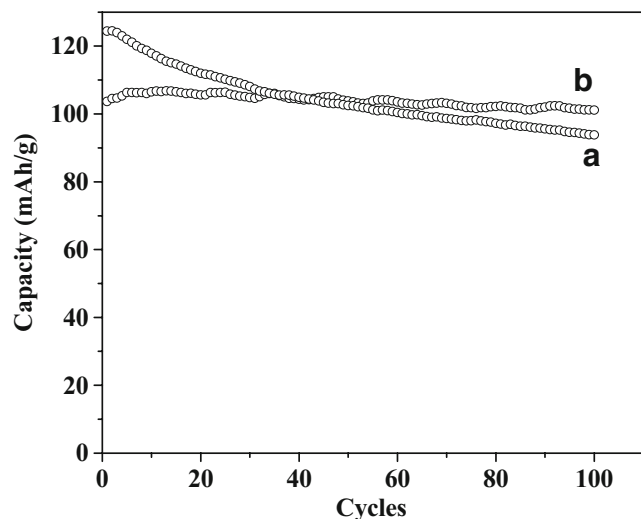**Fig. 4** Cross-sectional TEM image of **a** pure $LiMn_2O_4$ and **b** modified $LiMn_2O_4$

b

c

Fig. 2 SEM images of **a** pure $LiMn_2O_4$, **b** the mixture of $LiMn_2O_4$ and ZnO, (**c**) modified $LiMn_2O_4$

a

b

Fig. 5 Discharge curves of **a** pure $LiMn_2O_4$ and **b** modified $LiMn_2O_4$ before and after storage at 60 °C for a week

electrolyte solution because of the coated $ZnMn_2O_4$ shell on the surface of $LiMn_2O_4$ particle.

Pure $LiMn_2O_4$ powders (100 mg) and modified $LiMn_2O_4$ powders (100 mg) were soaked in 50 ml 1 M $LiPF_6$ EC/DEC/EMC (1:1:1 by volume ratio) under argon for 2 months, respectively. After soaking, the lithium manganese oxides were washed by ethanol and separated from the electrolyte with a filter paper. The amount of dissolved Mn ions in the electrolyte was analyzed by inductively coupled plasma. The Mn content for pure $LiMn_2O_4$ and modified $LiMn_2O_4$ are 481 and 23 $\mu g\ ml^{-1}$, respectively. The results reveal that the shell $ZnMn_2O_4$ can effectively minimize the Mn dissolution into the electrolyte, which is agreement with the result of Fig. 5.

Figure 6 compares the variation of specific capacity with cycle number for pure $LiMn_2O_4$ and modified $LiMn_2O_4$ at 0.5 C rate, in the 3.5–4.3 V ranges. The pure $LiMn_2O_4$ with

Fig. 6 Cycling behavior of **a** pure $LiMn_2O_4$ and **b** modified $LiMn_2O_4$
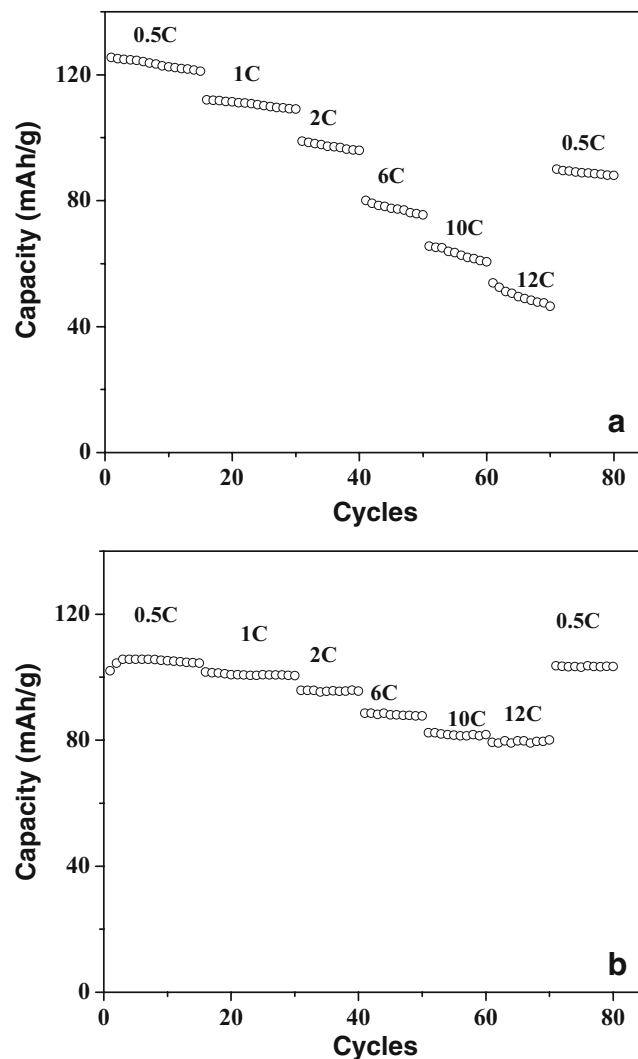
Fig. 7 The capacity vs. cycle number at different discharge rates: **a** pure $LiMn_2O_4$ and **b** modified $LiMn_2O_4$

initial capacity of 124.4 mAh g^{-1} declined rapidly as cycling, only remained 74.6% of its initial capacity after 100 cycles, which is about 0.306 mAh g^{-1} per cycle, while the capacity loss of modified LiMn$_2$O$_4$ at the 100th cycle, with about 0.052 mAh g^{-1} per cycle, is 4.9% of the maximum capacity that is 106.3 mAh g^{-1}. Obviously, the capacity retention of modified LiMn$_2$O$_4$ is remarkably enhanced.

Figure 7 presents the rate capability performance of pure LiMn$_2$O$_4$ and modified one at charge–discharge rates ranging from C/2 to 12C. Clearly, the modified LiMn$_2$O$_4$ maintained a steady discharge capacity as the charge–discharge rate increases, while the pure LiMn$_2$O$_4$ showed a rapidly decline at each charge–discharge rate, especially at high rates. For both pure LiMn$_2$O$_4$ and modified LiMn$_2$O$_4$, the discharge capacity decreased with the increase of charge–discharge rate (C/2–12C rate), which is caused by the low diffusion rate of the lithium ions in the LiMn$_2$O$_4$ particles; however, the decrease of discharge capacity of modified LiMn$_2$O$_4$ was much smaller than that of the pure one. As the charge–discharge rates were reduced from 12C to C/2, the pure LiMn$_2$O$_4$ only maintained 74.3% of its capacity on the 15th cycle at the same rate, while modified LiMn$_2$O$_4$ showed a very little capacity fading.

As described in introduction, capacity loss during cycling is related to Mn dissolution into the electrolyte solution. After being modified, LiMn$_2$O$_4$ diminished the direct contact with the electrolyte because of the ZnMn$_2$O$_4$ shell on the surface of LiMn$_2$O$_4$ particles. Therefore, our modification enhances the cycling performance of spinel LiMn$_2$O$_4$.

Conclusions

In this paper, we present a simple routine to the preparation of ZnMn$_2$O$_4$ shell-coated LiMn$_2$O$_4$ that shows excellent electrochemical performance. Because of the formation of ZnMn$_2$O$_4$ shell on the surface of spinel LiMn$_2$O$_4$ particles, the discharge curves of modified LiMn$_2$O$_4$ before and after storage at 60 °C for a week comparison with that of pure one shows that our modification diminishes the Mn dissolution into the electrolyte solution, which significantly improved the cycling performance of spinel LiMn$_2$O$_4$.

References

1. Singh D, Kim WS, Craciun V, Hofmann H, Singh RK (2002) Appl Surf Sci 197–198:516
2. Ein EY, Urian RC, Wen W, Mukerjee S (2005) Electrochim Acta 50:1931
3. Jang DH, Shin YJ, Oh SM (1996) J Electrochem Soc 143:2204
4. Li C, Zhang HP, Fu LJ, Liu H, Wu YP, Rahm E, Holze R, Wu HQ (2006) Electrochim Acta 51:3872
5. Xia YY, Sakai T, Fujieda T, Yang XQ, Sun X, McBreen J, Yoshio M (2001) J Electrochem Soc 148:A723
6. Arbizzani C, Balducci A, Mastragostino M, Rossi M, Soav F (2003) J Power Sources 119–121:695
7. Ha HW, Yun NJ, Kim K (2007) Electrochim Acta 52:3236
8. Chan HW, Duh JG, Sheen SR (2006) Electrochim Acta 51:3645
9. Yoshio M, Xia YY, Kumada NK, Ma SH (2001) J Power Sources 101:79